Graph Annotations in Modeling Complex Network Topologies

Xenofontas Dimitropoulos
IBM Research, Zürich
xed@zurich.ibm.com

Dmitri Krioukov
CAIDA/UCSD
dima@caida.org

Amin Vahdat
UCSD
vahdat@cs.ucsd.edu

George Riley
Georgia Tech
riley@ece.gatech.edu

ABSTRACT

The coarsest approximation of the structure of a complex network, such as the Internet, is a simple undirected unweighted graph. This approximation, however, loses too much detail. In reality, objects represented by vertices and edges in such a graph possess some non-trivial internal structure that varies across and differentiates among distinct types of links or nodes. In this work, we abstract such additional information as network *annotations*. We introduce a network topology modeling framework that treats annotations as an extended correlation profile of a network. Assuming we have this profile measured for a given network, we present an algorithm to rescale it in order to construct networks of varying size that still reproduce the original measured annotation profile.

Using this methodology, we accurately capture the network properties essential for realistic simulations of network applications and protocols, or any other simulations involving complex network topologies, including modeling and simulation of network evolution. We apply our approach to the Autonomous System (AS) topology of the Internet annotated with business relationships between ASs. This topology captures the large-scale structure of the Internet. In depth understanding of this structure and tools to model it are cornerstones of research on future Internet architectures and designs. We find that our techniques are able to accurately capture the structure of annotation correlations within this topology, thus reproducing a number of its important properties in synthetically-generated random graphs.

Categories and Subject Descriptors

C.2.1 [**Network Architecture and Design**]: Network topology; C.2.5 [**Local and Wide-Area Networks**]: Internet; G.3 [**Probability and Statistics**]: Distribution functions, multivariate statistics, correlation and regression analysis; G.2.2 [**Graph Theory**]: Network problems

General Terms

Measurement, Design, Theory

Keywords

Annotations, AS relationships, complex networks, topology

1. INTRODUCTION

Simulations of new network protocols and architectures are pointless without realistic models of network structure and evolution. Performance of routing [26], multicast [34], and other protocols depends crucially on network topology. Simulations of these protocols with inaccurate topology models can thus result in misleading outcomes.

Inaccuracies associated with representing complex network topologies as simple undirected unweighted graphs come not only from potential sampling biases in topology measurements [27, 10, 11], but also from neglecting link and node *annotations*. By annotations we mean various types of links and nodes that abstract their intrinsic structural and functional differences to a certain degree. For example, consider the Internet topology at the Autonomous System (AS) level. Here, link annotations may represent different business relationship between ASs, e.g., customer-to-provider, peer-to-peer, etc. [13], while node annotations may represent different types of ASs, e.g., large or small Internet Service Providers (ISPs), exchange points, universities, customer enterprises, etc. [15]. In router-level Internet topologies, link annotations can be different transmission speeds, latencies, packet loss rates, etc. One can also differentiate between distinct types of links and nodes in other networks, such as social, biological, or transportation networks. In many cases, simply reproducing the structure of a given network is insufficient; we must also understand and reproduce domain-specific annotations.

We propose network annotations as a general framework to provide the next level of detail describing the "microscopic" structure of links and nodes. Clearly, since links and nodes are constituents of a global network, increasing description accuracy at the "microscopic" level will also increase overall accuracy at the "macroscopic" level as well. That is, including appropriate per-node or per-link annotations will allow us to capture and reproduce more accurately a variety of important global graph properties. In the AS topology case, for example, instead of considering only shortest paths, we will be able to study the structure of paths that respect constraints imposed by routing policies and AS business relationships.

Higher accuracy in approximating network structure is desirable not only for studying applications and protocols that depend on such structure, but also for modeling network evolution. For example, realistic Internet AS topology

growth models should be based on economic realities of the Internet since AS links are nothing but reflections of AS contractual relationships, i.e., results of business decisions made by organizations that the corresponding ASs represent. Therefore, economy-based AS topology models naturally produce links annotated with AS relationships. AS relationship annotations are thus intrinsic to such models.

Network annotations should also be useful for researchers studying only those networks that preserve some domain-specific constraints, thus avoiding "too random" networks that violate these constraints. Examples of such "technological" constraints for router topologies include maximum node degree limits, specific relationships between node degree and centrality, etc. [28]. In this context, we note that any node or link attributes, including their degrees and centrality, are forms of annotations. Therefore, one can use the network annotation framework to introduce domain-specific or any other constraints to work with network topologies narrowed down to a specific class. We also note that the network annotation framework is sufficiently general to include directed and weighted networks as partial cases, since both link directions and weights are forms of annotations.

After reviewing, in Section 2, past work on network topology modeling and generation, which largely ignores annotations, we make the following contributions in this paper:

- In Section 3, we demonstrate the importance of network annotations using the specific example of AS business relationships in the Internet.
- In Section 4, we introduce a general network annotation formalism and apply it to the Internet AS topology annotated with AS business relationships.
- In Section 5, we formulate a general methodology and specific algorithms to: i) rescale the annotation correlation profile of the observed AS topology to arbitrary network sizes; and ii) construct synthetic networks reproducing the rescaled annotation profiles. While we discuss our graph rescaling and construction techniques in the specific context of AS topologies, these techniques are generic and can be used for generating synthetic annotated networks that model other complex systems.
- In Section 6, we evaluate the properties of the resulting synthetic AS topologies and show that they recreate the annotation correlations observed in real annotated AS topologies as well as other important properties directly related to common metrics used in simulation and performance evaluation studies.

We conclude by outlining some implications and directions for future work in Section 7.

2. RELATED WORK

A large number of works have focused on modeling Internet topologies and on developing realistic topology generators. Waxman [44] introduced the first topology generator that became widely known. The Waxman generator was based on the classical (Erdős-Rényi) random graph model [18]. After it became evident that observed networks have little in common with classical random graphs, new generators like GT-ITM [46] and Tiers [17] tried to mimic the perceived hierarchical network structure and were consequently called *structural*. In 1999, Faloutsos *et al.* [19] discovered that the degree distributions of router- and AS-level topologies of the Internet followed a power law. Structural generators failed to reproduce the observed power laws. This failure led to a number of subsequent works trying to resolve the problem.

The existing topology models capable of reproducing power laws can be roughly divided into the following two classes: causality-aware and causality-oblivious. The first class includes the Barabási-Albert (BA) [2] preferential attachment model, the Highly Optimized Tolerance (HOT) model [6], and their derivatives. The BRITE [32] topology generator belongs to this class, as it employs preferential attachment mechanisms to generate synthetic Internet topologies. The models in this class grow a network by incrementally adding nodes and links to a graph based on a formalized network evolution process. One can show that both BA and HOT growth mechanisms produce power laws.

On the other hand, the causality-oblivious approaches try to match a given (power-law) degree distribution without accounting for different forces that might have driven evolution of a network to its currently observed state. The models in this class include random graphs with given expected [9] and exact [1] degree sequences, Markov graph rewiring models [31, 23], and the Inet [45] topology generator. Recent work by Mahadevan *et al.* introduced the dK-series [29] extending this class of models to account for node degree correlations of arbitrary order. Whereas the dK-series provides a set of increasingly accurate descriptions of network topologies represented as graphs, network annotations are another, independent and "orthogonal" to dK-series, way to provide more accurate and complete information about actual complex systems that these graphs represent.

Frank and Strauss first formally introduced the annotated (colored) random Markov graphs in [20]. In their definition, every edge is colored by one of T colors. More recently, Söderberg suggested a slightly different definition [42], where every half-edge, i.e., stub, is colored by one of T colors. Every edge is thus characterized by a pair of colors. This definition is very generic. It includes uncolored and standard colored [20] random graphs, random vertex-colored graphs [40][1], and random directed graphs [5] as partial cases. Söderberg considers some analytic properties of the ensemble of these random colored graphs in [41]. In [43], he observes strong similarities between random graphs colored by T colors and random Feynman graphs representing a perturbative description of a T-dimensional system from quantum or statistical mechanics.

Recent works on annotation techniques specific to AS graphs include [12] and [8]. The GHITLE [12] topology generator produces AS topologies with c2p and p2p annotations based on simple design heuristics and user-controlled parameters. The work by Chang *et al.* [8] describes a topology evolution framework that models ASs' decision criteria in establishing c2p and p2p relationships. Our methodology is different in that it explores the orthogonal, causality-oblivious approach to modeling link annotations. Its main advantage is that it is applicable to modeling any type of complex networks.

[1]Random graphs with colored nodes are a partial case of random graphs with hidden variables [3].

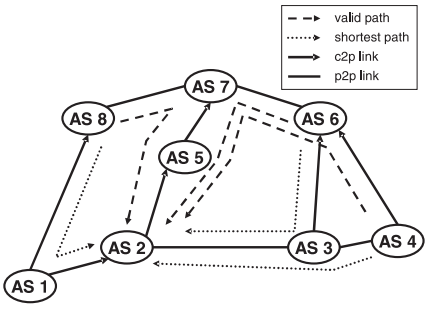

Figure 1: Example AS topology annotated with AS relationships. The dotted lines represent shortest paths between ASs 4, 6 and 8 to AS 2. The dashed lines represent policy compliant paths from the same sources to the same destination.

3. AS RELATIONSHIPS AND WHY THEY MATTER

In this section, we introduce our specific example of network annotations—AS relationships. We first describe what AS relationships represent and then discuss the results of simple simulation experiments showing why preserving AS relationship information is important.

AS relationships are annotations of links of the Internet AS-level topology. They represent business agreements between pairs of AS neighbors. There are three major types of AS relationships: 1) customer-to-provider (c2p), connecting customer and provider ASs; 2) peer-to-peer (p2p), connecting two peer ASs; and 3) sibling-to-sibling (s2s), connecting two sibling ASs. This classification stems from the following BGP route export policies, dictated by business agreements between ASs:

- exporting routes to a provider or a peer, an AS advertises its local routes and routes received from its customer ASs only;
- exporting routes to a customer or a sibling, an AS advertises all its routes, i.e., its local routes and routes received from all its AS neighbors.

Even though there are only two distinct export policies, they lead to the three different AS relationship types when combined in an asymmetric (c2p) or symmetric (p2p or s2s) manner.

If all ASs strictly adhere to these export policies, then one can easily check [21] that every AS path must be of the following *valley-free* or *valid* pattern: zero or more c2p links, followed by zero or one p2p links, followed by zero or more p2c links, where by 'p2c' links we mean c2p links in the direction from the provider to the customer.

Routing policies reflect business agreements and economic incentives. For this reason, they are deemed more important than quality of service and other criteria. As a result, suboptimal routing and inflated AS paths often occur. Gao and Wang [22] used BGP data to measure the extent of AS path inflation in the Internet. They found that at least 45% of the AS paths observed in BGP data are inflated by at least one AS hop and that AS paths can be inflated by as long as 9 AS hops.

Taking into account such inflation effects is important for meaningful and realistic simulation studies. For example, consider the AS topology in Figure 1, which is a small part of the real (measured) AS topology annotated with AS relationships inferred using heuristics in [14]. Directed links represent c2p relationships that point towards the provider and undirected links represent p2p relationships. If we ignore AS relationships then the shortest paths from ASs 4, 6, and 8 to AS 2 are shown with dotted lines. On the other hand, if we account for AS relationships these paths are no longer valid. In particular, the path 4→3→2 transverses two p2p links; the path 6→3→2 transverses a p2c link followed by a p2p link; and the path 8→1→2 transverses a c2p link after having gone through a p2c link. As all these paths are not valid, they are not used in practice. The paths actually used are the policy compliant paths marked with dashed lines.

Table 1: Total number of paths for each AS with AS relationships enabled and AS relationships disabled.

AS number		1	2	3	4	5	6	7	8
Number of paths	AS relationships disabled	12	13	16	15	13	15	15	13
	AS relationships enabled	12	9	10	8	8	7	9	6

In other words, the first effect of taking AS relationships into account is that paths become longer than the corresponding shortest paths. From a performance perspective, longer paths can affect metrics such as end-to-end (e2e) delay, server response time, jitter, convergence time, and others.

To illustrate this effect, we simulated the topology in Figure 1 using BGP++ [16]. We used a single router per AS and configured appropriate export rules between ASs according to the guidelines discussed above. We set the delay of each link to 10 milliseconds and the bandwidth to 400kbps. Then, we configured exponential on/off traffic sources at ASs 4, 6 and 8 that send traffic to AS 2 at a rate of 500kbps. We run the simulation for 120 seconds; for the first 100 seconds we waited for routers to converge[2] and at the 100th second we started the traffic sources. We then measured the e2e delay between the sources and the destination with AS relationships disabled and enabled.

In Figure 2 we depict the cumulative distribution function (CDF) of the e2e delays for the both cases. We first notice that the CDF with AS relationships enabled shifts to the right, which means that there is a significant increase in the e2e delay. In particular, the average e2e delay with AS relationships enabled is 0.853 seconds, whereas without AS relationships it drops to 0.389 seconds. Besides the decrease in the e2e delay, we see that the CDF with AS relationships is much smoother than the other CDF, which exhibits a step-wise increase. The reason for that difference is that in the former case we have more flows sharing multiple queues and, consequently, more diverse queue dynamics, while in the latter case, almost all paths are disjoint, leading to mostly fixed e2e delays. The observed difference signifies that the e2e delay with AS relationships enabled exhibits a much higher variability compared to the case with AS relationships ignored. This difference in variability is likely to affect other performance metrics like jitter and router buffer occupancy.

Another consequence of policy-constrained routing is that ASs have fewer alternative AS paths. For example, in Fig-

[2]Typically routers take much less than 100 seconds to converge, but to be conservative we used a longer period.

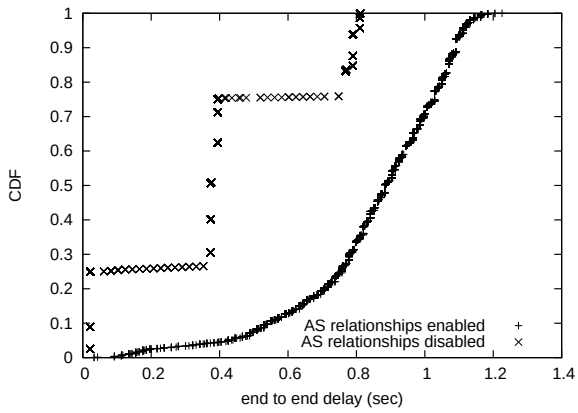

Figure 2: CDF of e2e delay between traffic sources and destination.

Table 2: Average bandwidth per flow with AS relationships enabled or disabled.

Flow		4 → 2	6 → 2	8 → 2
Bandwidth (Kbps)	AS relationships disabled	202	196	397
	AS relationships enabled	113	164	121

ure 1 when ignoring AS relationships AS 7 has three (one through each neighbor) disjoint paths to reach destination 2. One the other hand, with AS relationships enabled, AS 7 has only one possible path through AS 5, since the other two paths are not valid. In Table 1, we show the total number of paths we found in the BGP tables of the eight ASs in our simulations. The consistent decrease in the number of paths when AS relationships are enabled highlights that ignoring AS relationships increases the path diversity of the ASs in a simulation. Path diversity is an important property related to network robustness, vulnerability to attacks, links and router failures, load balancing, multi-path routing, convergence of routing protocols, and others.

Yet another effect of policy routing is different distribution of load on ASs and AS links. Indeed, due to the smaller number of available AS paths, compared to shortest path routing, some nodes and links are likely to experience greater traffic load. For example, in Figure 1 the dashed paths share the links from AS 7 to AS 5. On the other hand, when assuming shortest path routing the three paths are mostly disjoint: only one link, the link between AS 3 and AS 2, is shared by two flows. Thus, AS links and nodes will receive greater load, compared to the case with AS relationships ignored. Higher load is likely to produce more packet loss, increased delay, congestion, router failures, and other undesirable effects. In Table 2 we list the average bandwidth in our simulations for each of the three flows with and without AS relationships enabled. We find that because of the increased load on the links between AS 7 and AS 5 the average bandwidth of the three flows decreases substantially.

To summarize this section, we have provided three examples showing that ignoring AS relationship annotations leads to inaccuracies, which make the corresponding properties look "better" than they are in reality. Indeed, if AS relationships are ignored, then:

- paths are shorter than in reality;
- path diversity is larger than in reality; and
- traffic load is lower than in reality.

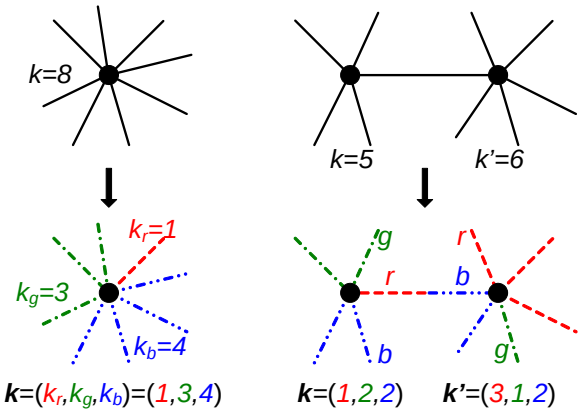

Figure 3: The $1K$- and $2K$-annotations. Three different stub colors are represented by dashed (color *red*), dash-dotted (color *green*), and dash-double-dotted (color *blue*) lines.

4. NETWORK TOPOLOGY ANNOTATIONS

In this section we first introduce our general formalism to annotate network topologies. We then show how this formalism applies to our example of the AS-level Internet topology annotated with AS relationships.

4.1 General formalism

Our general formalism is close to random colored graph definitions from [42] and borrows parts of the convenient dK-series terminology from [29].

We define the annotated network as a graph $G(V, E)$, $|V| = n$ and $|E| = m$, such that all $2m$ edge-ends (stubs) of all m edges in E are of one of several colors c, $c = 1 \dots C$, where C is the total number of stub colors. We also allow for node annotations by an independent set of node colors $\theta = 1 \dots \Theta$. We do not use node annotations in this paper and we do not include them in the expressions below in order to keep them clearer. It is however trivial to add node annotations to these expressions.

Compared to the non-annotated case when the node degree is fully specified by an integer value k of the number of stubs attached to the node, we now have to list the numbers of attached stubs of each color to fully describe the node degree. Instead of scalar k, we thus have the node degree vector

$$\mathbf{k} = (k_1, \dots, k_C),$$

which has C components k_c, each specifying the number of c-colored stubs attached to the node, cf. the left side of Figure 3. The L^1-norm of this vector yields the node degree with annotations ignored,

$$k = |\mathbf{k}|_1 = \sum_{c=1}^{C} k_c. \qquad (1)$$

The number $n(\mathbf{k})$ of nodes of degree $\mathbf{k}$ defines the node degree distribution,

$$\frac{n(\mathbf{k})}{n} \xrightarrow[n\to\infty]{} P(\mathbf{k}), \qquad (2)$$

in the large-graph limit. We can think of $n(\mathbf{k})$ as a non-normalized form of $P(\mathbf{k})$. From the statistical perspective, the $n(\mathbf{k})$ ($P(\mathbf{k})$) distribution is a multivariate distribution. Its C marginal distributions are the distributions of node degrees of each color c:

$$n(k_c) = \sum_{\mathbf{k}' \,\big|\, k'_c = k_c} n(\mathbf{k}'), \tag{3}$$

where the summation is over all vectors $\mathbf{k}'$ such that their c's component is equal to k_c. The degree distribution $n(\mathbf{k})$ thus represents per-node correlations of degrees of different colors. Following the terminology in [29], we call the node degree distribution $n(\mathbf{k})$ ($P(\mathbf{k})$) the $1K$-*annotated distribution*.

We then define the $2K$-*annotated distribution* as correlations of annotated degrees of connected nodes, or simply as the number of edges that have stub of color c connected to a node of degree $\mathbf{k}$ and the other stub of color c' connected to a node of degree $\mathbf{k}'$, $n(c, \mathbf{k}; c', \mathbf{k}')$. See the right side of Figure 3 for illustration.

As in the non-annotated case, the $2K$-distribution yields a more exhaustive statistics about the annotated network topology and fully defines the $1K$-distribution. To see that, we introduce the following notations:

$$\begin{aligned} \tilde{\mathbf{k}} &= (c, \mathbf{k}), \\ \tilde{\mathbf{k}}' &= (c', \mathbf{k}'), \\ \mu(c, c') &= 1 + \delta(c, c'), \\ \mu(\mathbf{k}, \mathbf{k}') &= 1 + \delta(\mathbf{k}, \mathbf{k}'), \\ \mu(\tilde{\mathbf{k}}, \tilde{\mathbf{k}}') &= 1 + \delta(\tilde{\mathbf{k}}, \tilde{\mathbf{k}}'), \end{aligned}$$

where $\delta(x, x')$ is the standard Kronecker delta:

$$\delta(x, x') = \begin{cases} 1 & \text{if } \; x = x', \\ 0 & \text{otherwise}, \end{cases}$$

and x is either c, $\mathbf{k}$, or $\tilde{\mathbf{k}}$. With these notations, one can easily check that the normalized $2K$-annotated distribution is

$$P(\tilde{\mathbf{k}}, \tilde{\mathbf{k}}') = n(\tilde{\mathbf{k}}, \tilde{\mathbf{k}}')\mu(\tilde{\mathbf{k}}, \tilde{\mathbf{k}}')/(2m), \tag{4}$$

the number of edges of any pair of colors connecting nodes of degrees $\mathbf{k}$ and $\mathbf{k}'$ is

$$n(\mathbf{k}, \mathbf{k}') = \sum_{c, c'} n(\tilde{\mathbf{k}}, \tilde{\mathbf{k}}')\mu(\tilde{\mathbf{k}}, \tilde{\mathbf{k}}')/\mu(\mathbf{k}, \mathbf{k}'),$$

the normalized form of this distributions is

$$P(\mathbf{k}, \mathbf{k}') = n(\mathbf{k}, \mathbf{k}')\mu(\mathbf{k}, \mathbf{k}')/(2m),$$

and the $1K$-distribution is given by

$$n(\mathbf{k}) = \sum_{\mathbf{k}'} n(\mathbf{k}, \mathbf{k}')\mu(\mathbf{k}, \mathbf{k}')/k, \tag{5}$$

$$P(\mathbf{k}) = \frac{\bar{k}}{k} \sum_{\mathbf{k}'} P(\mathbf{k}, \mathbf{k}'), \tag{6}$$

where $\bar{k} = 2m/n$ is the average degree. The last two expressions show how one can find the $1K$-annotated distribution given the $2K$-annotated distribution, and they look exactly the same as in the non-annotated case [29], except that we have vectors $\mathbf{k}, \mathbf{k}'$ instead of scalars k, k'.

The dK-annotated distributions with $d > 2$ [29] can be defined in a similar way.

4.2 The AS relationship annotations

In the specific case of the AS-level Internet topology that interests us in this paper, we have just three colors: customer, provider, and peer.[3] We assign the following numeric values to represent these three colors:

$$c = \begin{cases} 1 & \text{customer}, \\ 2 & \text{provider}, \\ 3 & \text{peer}. \end{cases}$$

These three stub annotations come under the following two constraints defining the only two types of edges that we have: 1) *c2p edges*: if one stub of an edge is customer, then the other stub of the same edge is provider, and vice versa; and 2) *p2p edges*: if one stub of an edge is peer, then the other stub of the same edges is also peer. The c2p edges are thus asymmetric, i.e., a generalization of directed edges, while the p2p edges are symmetric, i.e., a generalization of bi-directed or undirected edges.

While the $2K$-annotated distribution $n(\tilde{\mathbf{k}}, \tilde{\mathbf{k}}')$ contains the most exhaustive information about the network topology, it has too many (seven) independent arguments. As a result, the full $2K$-annotated statistics is extremely sparse, which makes it difficult to model and reproduce directly. We thus have to find some summary statistics of $n(\tilde{\mathbf{k}}, \tilde{\mathbf{k}}')$ that we can model in practice. For each concrete complex network type, these summary statistics might be different. Given measurement data for a specific complex network, one would usually have to start with identifying a meaningful set of summary statistics of the $2K$-annotated distribution, and then proceed from there. At the same time, we believe that as soon as the $2K$-annotated distribution fully defines an observed complex network, i.e., the network is $2K$-annotated-random [29], one can generally use the set of summary statistics that we found necessary and sufficient to reproduce in order to model correctly the Internet AS topology. In the rest of this section, we list these statistics and describe the specific meanings that they have in the AS topology case.

Degree distribution (DD). This statistics is the traditional non-annotated degree distribution $n(k)$, where k is as in eq. (1). The DD tells us how many ASs of each total degree k are in the network.

Annotation distributions (ADs). The DD of an AS topology does not convey any information about the AS relationships. The initial step to account for this information is to reproduce the distributions of ASs with specific numbers of attached customer, provider, or peer stubs. These annotation distributions (ADs) are the marginal distributions $n(k_c)$, $c = 1, 2, 3$, of the $1K$-annotated distribution. They are given by eq. (3). If k_1 (k_2) customer (provider) stubs attach to an AS, then this AS has exactly k_1 (k_2) providers (customers), since the c2p edges are asymmetric. Consequently, the ADs $n(k_1)$ and $n(k_2)$ tell us how many ASs with the specific numbers of providers and, respectively, customers the network has. Since the p2p edges are symmetric, the AD $n(k_3)$ is the distribution of ASs with specific numbers of peers.

Annotated degree distribution (ADD). The ADs do not tell us anything about the correlations among anno-

[3]We ignore sibling relationships, since they typically account for a very small fraction of the total number of edges. As found in [13], the number of s2s edges is only 0.46% of the total number of edges in the AS-level Internet.

tated degrees of the same node, i.e., how many customers, providers, *and*, simultaneously, peers a specific AS has. Correlations of this type are fully described by the $1K$-annotated distribution in eq. (2), which we also call the annotated degree distribution (ADD). These correlations are present in the Internet. For example, large tier-1 ISPs typically have a large number of customers, i.e., large k_2, no providers, i.e., zero k_1, and a small number of peers, i.e., small k_3. On the other hand, medium-size ISPs tend to have a small set of customers, several peers, and few providers. Ignoring the ADD while generating synthetic graphs can lead to artifacts like high-degree nodes with many providers—a property obviously absent in the real Internet.

Joint degree distributions (JDDs). While the ADD contains the full information about degree correlations "at nodes," it does not tell us anything about degree correlations "across links," while the latter type of correlations is also characteristic for the Internet. For example, large tier-1 ISPs typically have p2p relationships with other tier-1 ISPs, not with much smaller ISPs, while small ISPs have p2p links with other small ISPs. In other words, p2p links usually connect ASs of similar degrees, i.e., $k \sim k'$. Similarly, c2p links tend to connect low-degree customers to high-degree providers, i.e., $k \ll k'$. If we ignore these correlations, we can synthesize graphs with inaccuracies like p2p links connecting ASs of drastically dissimilar degrees. To reproduce these correlations, we work with the following summary statistics of the $2K$-annotated distribution in eq. (4):

$$n_{c2p}(k,k') = \sum_{\mathbf{k},\mathbf{k}' \;|\; |\mathbf{k}|_1=k,\, |\mathbf{k}'|_1=k'} n(1,\mathbf{k};2,\mathbf{k}'), \quad (7)$$

$$n_{p2p}(k,k') = \sum_{\mathbf{k},\mathbf{k}' \;|\; |\mathbf{k}|_1=k,\, |\mathbf{k}'|_1=k'} n(3,\mathbf{k};3,\mathbf{k}'), \quad (8)$$

where the summation is over such vectors $\mathbf{k}$ and $\mathbf{k}'$ that their L^1-norms are k and k' respectively. The first expression gives the number of c2p links that have their customer stub attached to a node of total degree k and provider stub attached to a node of total degree k'. The second expression is the number of p2p links between nodes of total degrees k and k'. In other words, these two objects are the joint degree distributions (JDDs) for the c2p and p2p links.

In summary, we work with the four types of distributions, i.e., DD, ADs, ADD, and JDDs, that allow two types of classification:

1. **Univariate vs. multivariate distributions:**
   (a) Univariate. The ADs and DD are distribution of only one random variable.
   (b) Multivariate. The ADD and JDDs are joint distribution of three and two random variables. The marginal distribution of these variables are the ADs, cf. eq. (3), and DD, cf. eqs. (7,8), respectively.
2. **1K- vs. 2K-summary statistics:**
   (a) $1K$-derived. The DD, ADs, and ADD are fully defined by the $1K$-annotated distribution: that is, we do not need to know the $2K$-annotated distribution to calculate the distributions in this class.
   (b) $2K$-derived. The JDDs are fully defined only by the $2K$-annotated distribution. Note that it also defines the $1K$-annotated distribution via eqs. (5,6).

5. GENERATING ANNOTATED AS GRAPHS

In this section we describe how we generate synthetic annotated AS graphs of arbitrary sizes. We want our synthetic graphs to reproduce as many important properties of the original measured topology as possible. For this purpose we decide to explicitly model and reproduce the summary statistics of the $2K$-annotated distribution from Section 4.2, because [29] showed that by reproducing $2K$-distributions, one automatically captures a long list of other important properties of AS topologies. In other words, the task of generating synthetic annotated topologies becomes equivalent to the task of generating random annotated graphs that reproduce the summary statistics of the $2K$-annotated distribution of the measured AS topology.

We wish to be able to generate synthetic topologies of different sizes, but the $2K$-summary statistics defined in Section 4.2 are all bound to a specific graph size. Therefore, in order to generate arbitrarily-sized graphs, we need first to rescale the $2K$-summary statistics from the original to target graph sizes. We say that an empirical distribution is *rescaled* with respect to another empirical distribution, if the both distributions are defined by two different finite collections of random numbers drawn from the same continuous distribution. For example, the distributions of node scalar (or vector) degrees in two different graphs are rescaled with respect to each other if these degrees are drawn from the same continuous univariate (or multivariate) probability distribution. We say that a $2K$-annotated graph is *rescaled* with respect to another $2K$-annotated graph, if all the $2K$-summary statistics of the first graphs are rescaled with respect to the corresponding $2K$-summary statistics of the second graph. This definition of rescaling is equivalent to assuming that for each summary statistic, the same distribution function describes the ensemble of empirical distributions of the statistic in past, present, and future Internet topologies. In other words, we assume that the $2K$-annotated correlation profile of the Internet AS topology is an invariant of its evolution. This assumption is realistic, as discussed, for example, in [36], where it is shown that the non-annotated $1K$- and $2K$-distributions of the Internet AS topology have stayed approximately the same during all the years (more than a decade) of the existing data time span.

To illustrate what we mean by *rescaling*, consider the empirical distribution of peer degrees, i.e., the AD $n(k_3)$, in the measured AS topology annotated with AS relationships in Figure 4(a). The figure shows the empirical complementary cumulative distribution function (CCDF) for peer-degrees of 19,036 nodes, i.e., 19,036 numbers of peer stubs attached to a node, and the largest such number is 448. The continuous probability distribution of Figure 4(b) approximates the empirical distribution in Figure 4(a). Figures 4(c), 4(d), and 4(e) show the CCDFs of three collections of 5,000, 20,000, and 50,000 random numbers drawn from the probability distribution in Figure 4(b). According to our definition of rescaling, the distributions in Figures 4(c), 4(d), and 4(e) are rescaled with respect to the distribution of Figure 4(a). We see that all the empirical distributions have the same overall shape, but differ in the total number of samples and in the maximum values within these sam-

ple collections. Distributions with larger maximums correspond, as expected, to bigger collections of samples.

5.1 Overview of the approach

We now move to describing the details of our approach, which consists of the following three major phases:

1. **Extraction.**

   We first extract the empirical $2K$-summary distributions from available AS topology measurement data. We annotate links of the AS topology extracted from this data using existing AS relationship inference heuristics. This extraction step is conceptually simplest. On its output, we obtain the extracted $2K$-summary distributions that are all bound to the size of the measured AS graph.

2. **Rescaling.**

   (a) We use the extracted empirical distributions to find their continuous approximations. Referring to our example in Figure 4, this step corresponds to computing the continuous probability distribution in Figure 4(b) based on the empirical distribution in Figure 4(a).

   (b) We then use the computed probability distributions to rescale the empirical distributions obtained at the extraction step. We generate a desired, target number of random scalar or vector degree samples drawn from the corresponding probability distributions. The generated degree samples have empirical distributions that are rescaled with respect to the corresponding empirical distributions of the measured topology. Referring to our example in Figure 4, this step corresponds to generating the rescaled empirical distributions in Figures 4(c), 4(d), and 4(e) based on the probability distribution in Figure 4(b).

3. **Construction.**

   Finally, we develop algorithms to generate synthetic graphs that have their $2K$-summary distributions equal to given distributions, i.e., to the corresponding distributions obtained at the previous step. The generated graphs thus reproduce the rescaled replicas of the $2K$-annotated distribution of the original topology, but they are "maximally random" in all other respects.

In the rest of this section, we describe each of these phases in detail.

5.2 Extraction

We extract the AS topology from the RouteViews [38] data, performing some standard data cleaning, such as ignoring private AS numbers, AS sets, etc. [30] The resulting AS graph is initially non-annotated. To annotate it, we infer c2p and p2p relationships for AS links using the heuristics in [13]. We thus obtain the real Internet AS topology annotated with c2p and p2p relationships. Given this annotated topology, we straightforwardly calculate all the empirical $2K$-summary distributions that we have defined in Section 4.2.

While the extraction phase is conceptually and technically the simplest phase of the overall approach, it is its basis. Therefore the quality of the input Internet topology data is a natural concern. This data is known to exhibit a variety of vagaries, e.g., due to sampling biases [27, 10, 11]. However, our approach is oblivious with respect to data quality. It takes any available data, extracts the described statistics from it, and reproduces them, properly rescaled, in random synthetic graphs. A given input topology data set thus defines an ensemble of random graphs generated by our method. By construction, all graphs in this ensemble reproduce the described set of annotated distributions. In addition, in Section 6, we perform sensitivity analysis in order to see the strength of fluctuations of these and other basic graph metrics within an ensemble. The quality of these graph ensembles, in terms of how veraciously they reflect reality, will improve as the quality of available topology data improves in the future. In this paper, we simply illustrate our approach with the currently available topology data. The RouteViews [38] is just one of very few sources of such data [30]. We select it because it appears to be the most frequently cited Internet topology data source.

5.3 Rescaling

Our rescaling approach differs for univariate and multivariate distributions.

5.3.1 Rescaling univariate distributions

We recall from the end of Section 4.2 that we have the following two types of univariate distributions: the ADs and the DD. Here we describe how we rescale ADs. We note that we do not have to rescale the DD the same way. The reason is that our approach to rescaling the ADD, which we discuss below in Section 5.3.2, automatically takes care of rescaling the DD, since the ADD is the distribution of degree vectors and the DD is the distribution of the L^1-norms of these vectors, cf. eq. (1).

The first problem we face trying to compute a continuous approximation for a given finite empirical distribution is that we have to not only interpolate between points of the empirical distribution, but also extrapolate above its maximum value. For example, if we want to construct a synthetic graph bigger than the original, then we expect its maximum degree to be larger than the maximum degree in the original graph. Therefore we have to properly extrapolate the observed degree distribution beyond the observed maximum degree.

We solve this problem by fitting the univariate empirical distributions with *smoothing splines*. Spline smoothing is a non-parametric estimator of an unknown function represented by a collection of empirical data points. Spline smoothing produces a smooth curve passing through or near the data points. For example, the curve in Figure 4(b) is a smooth spline of the empirical distribution of Figure 4(a). Spline smoothing can also extrapolate the shape of an empirical function beyond the original data range.

Another reason to select spline smoothing is that it comes useful for fitting distributions that do not closely follow regular shapes, e.g., "clean" power laws. The ADs of the Internet topology do not necessarily have such regular shapes. For example, the distribution of the number of peers, i.e., the AD $n(k_3)$, has a complex shape that we found impossible to fit with any single-parametric distribution.

Among available implementations of spline smoothing techniques, we select the one in the `smooth.spline` method of

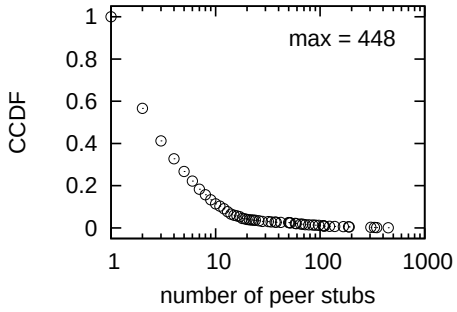

(a) Original distribution of 19,036 peer-degrees in the measured AS topology.

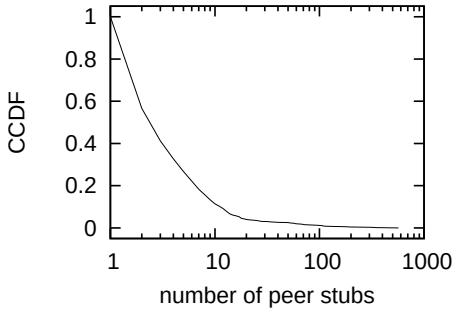

(b) Continuous distribution approximating the original one.

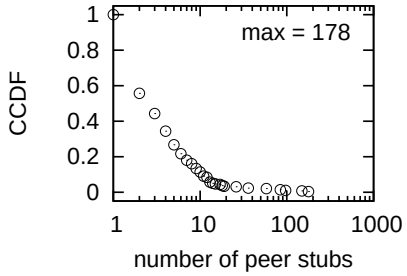

(c) Rescaled distribution of 5,000 samples.

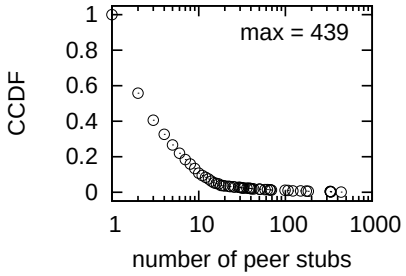

(d) Rescaled distribution of 20,000 samples.

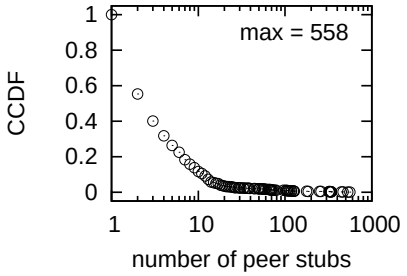

(e) Rescaled distribution of 50,000 samples.

Figure 4: Rescaling an empirical distribution. The distributions in the three bottom figures are rescaled with respect to the empirical distribution in the first figure. The distribution in the second figure is a continuous approximation of the distribution in the first figure and is used to generate the rescaled distributions in the bottom figures. For each discrete distribution, we show its maximum in the top-right corners of the plots.

the R project [37], a popular statistical computing package. The specific details of this technique are in [7].

We can approximate with splines either the CDFs or CCDFs[4] of the ADs obtained at the extraction step. We chose to fit the CCDFs rather than the CDFs because the former better capture the shapes of high-degree tails of our heavy-tailed ADs.

Another important detail is that we can define an empirical CCDF to be either a left- or right-continuous step function [24]. Usually an empirical CCDF at some point x is defined as the fraction of samples with values strictly larger than x, which means that the distribution is right-continuous and that the probability of a value larger than the observed maximum value is zero, whereas the probability of a value smaller than the observed minimum value is unspecified. For degree distributions, we know that the probability of a degree smaller than zero is zero,[5] but we do not know the probability of a degree larger than the maximum observed degree. For this reason, we decide to fit the left-continuous variants of empirical CCDFs, i.e., we define a CCDF at some point x as the fraction of samples with values greater than or equal to x.

Having the original ADs fitted with splines and assuming that our target graph size is N, we finally use the standard, inverse-CDF method to produce N random numbers that follow the continuous distributions given by the splines. Recall that the inverse-CDF method is based on the observation that if the CDF of N random numbers x_j, $j = 1 \ldots N$, closely follows some function $F(x)$, then the distribution of numbers $y_j = F(x_j)$ is approximately uniform in the interval $[0, 1]$. As its name suggests, the inverse-CDF inverts this observation and operates as follows [25]: given a target CDF $F(x)$ and a target size N of a collection of random samples, the method first generates N random numbers y_j uniformly distributed in $[0, 1]$ and then outputs numbers $x_j = F^{-1}(y_j)$, where $F^{-1}(y)$ is the inverse of CDF $F(x)$, i.e., $F^{-1}(F(x)) = x$. The CDF of numbers x_j closely follows $F(x)$. Figures 4(c), 4(d), and 4(e) show random numbers generated this way. These numbers follow the distribution in Figure 4(b). To compute values of inverse CDFs on N random numbers uniformly distributed in $[0, 1]$ in our case, we use the `predict.smooth.spline` method of the R project. Since the random numbers produced in this way are not, in general, integers, we convert them to integer degree values using the floor function. We have to use the floor and not the ceiling function because we work with left- rather than right-continuous distributions.

The outcome of the described process is three sets of N random numbers that represent N customer degrees d_1^j, N provider degrees d_2^j, and N peer degrees d_3^j of nodes in the target graph, $j = 1 \ldots N$. We denote the CDFs of these random numbers by $D_1(d_1)$, $D_2(d_2)$, and $D_3(d_3)$ respectively. By construction, these distributions are properly rescaled versions of the customer-, provider- and peer-annotation distributions (ADs) in the measured AS topology.

5.3.2 Rescaling multivariate distributions

Rescaling multivariate distributions is not as simple as rescaling univariate distributions. Our approach for rescaling univariate distributions is not practically applicable to rescaling multivariate distributions because it is difficult to fit distributions that have many variates and complex shapes. To rescale multivariate distributions, we use *copulas* [33], which are a statistical tool for quantifying correlations between several random variables. Compared to other well-known correlation metrics, such as Pearson's coefficient, copulas give not a single scalar value but a function of several arguments that fully describes complex, fine-grained details of the structure of correlations among the variables, i.e., their correlation profile.

According to Sklar's theorem [39], any p-dimensional multivariate CDF F of p random variables $\mathbf{k} = (k_1, \ldots, k_p)$ can be written in the following form:

$$F(\mathbf{k}) = H(\mathbf{u}), \tag{9}$$

where $\mathbf{u}$ is the p-dimensional vector composed of the F's marginal CDFs $F_m(k_m)$, $m = 1, \ldots, p$:

$$F_m(k_m) = F(\infty, \ldots, \infty, k_m, \infty, \ldots, \infty), \tag{10}$$

$$\mathbf{u} = (F_1(k_1), \ldots, F_p(k_p)). \tag{11}$$

The function H is called a copula and each of its marginal distributions is uniform in $[0, 1]$.

Copulas play a critical role at the following two steps in our approach for rescaling multivariate distributions. First, they allow us to split a multivariate distribution of the original, measured topology into two parts: the first part consists of the marginal distributions F_m, while the second part is their correlation profile, i.e., copula H. These two parts are independent. Therefore, we can *independently* rescale the marginal distributions and the correlation profile. This property tremendously simplifies the rescaling process. The marginals are univariate distributions that we rescale as in Section 5.3.1, while this section contains the details of how we rescale the correlation profile. We use copulas the second time to merge together rescaled marginals and their correlation profile to yield a rescaled multivariate distribution in its final form.

In Figure 5 we present a high-level overview of our approaches for rescaling univariate and multivariate distributions. To rescale an original empirical univariate distribution, we first approximate it with splines and then use these splines to generate random numbers. We split the process of rescaling an original empirical multivariate distribution into two independent rescaling sub-processes, i.e., rescaling the marginals and their copula. We rescale the marginals as any other univariate distributions. To rescale the copula, we re-sample measured correlation data as we describe below in this section. At the end of multivariate rescaling, we merge the rescaled marginals with the rescaled copula to yield a rescaled multivariate distribution. One can see from Figure 5 that multivariate rescaling is a "superset," in terms of actions involved, of univariate rescaling. The following three steps summarize the high-level description of our multivariate rescaling approach:

1. extract and rescale the univariate marginals of a multivariate distribution as described in Section 5.3.1 (boxes (a), (b), and (c) in Figure 5);
2. extract and rescale the copula of the multivariate distribution (boxes (d) and (e) in Figure 5); and
3. merge the rescaled marginals and copula yielding a rescaled multivariate distribution (box (f) in Figure 5).

[4]Recall that the CCDF of CDF $F(x)$ is $1 - F(x)$.

[5]For a given node, some but not all the degrees k_1, k_2, and k_3 can be equal to zero.

In the rest of this section, we provide the low-level details for the last two steps, using the ADD multivariate distribution as an example.

At Step 2, we compute a rescaled ADD copula as follows. The collected AS topology has n nodes, and for each node i, $i = 1 \dots n$, we record its degree vector $\mathbf{k}_i = (k_1^i, k_2^i, k_3^i)$ producing an n-sized set of degree triplets. We then perform statistical simulation on this set to produce another set of a desired size that has the same correlations as the measured data $\mathbf{k}_i$. Specifically, we re-sample, uniformly at random and with replacement, N degree triplets from the set of vectors $\mathbf{k}_i$, where N is the target size of our synthetic topology. We thus obtain an N-sized set of random triplets $\mathbf{k}_j$, $j = 1 \dots N$, and we denote their joint CDF by $F(\mathbf{k})$. By construction, the empirical distribution of triplets $\mathbf{k}_j$ has the same correlation profile as original triplets $\mathbf{k}_i$. This procedure corresponds for box (d) in Figure 5.

Next, see box (e) in Figure 5, we compute the empirical copula of distribution $F(\mathbf{k})$. By definition, the copula of $F(\mathbf{k})$ is simply the joint distribution of vectors $\mathbf{u}$ in eqs. (9,11). Therefore, we first compute the marginal CDFs $F_1(k_1)$, $F_2(k_2)$, and $F_3(k_3)$ as CDFs of the first, second, and third components of vectors $\mathbf{k}_j$:

$$u_m^j = F_m(k_m^j) = r_m^j/N, \quad m = 1, 2, 3, \tag{12}$$

where r_m^j is the rank (position number) of value k_m^j in the N-sized list of values k_m sorted in the non-decreasing order. Random triplets $\mathbf{u}_j = (F_1(k_1^j), F_2(k_2^j), F_3(k_3^j))$ are uniformly distributed in the cube $[0, 1]^3$, and their joint CDF $H(\mathbf{u})$, $\mathbf{u} = (F_1(k_1), F_2(k_2), F_3(k_3))$, is the empirical copula for distribution $F(\mathbf{k})$, cf. eq. (9), that describes the correlations among k_1, k_2, and k_3.

At Step 3, box (f) in Figure 5, we merge the rescaled marginals $D_m(d_m)$, $m = 1, 2, 3$, from Section 5.3.1 and copula $H(\mathbf{u})$ by computing the target graph degree triplets $\mathbf{q}_j = (q_1^j, q_2^j, q_3^j)$, $j = 1, \dots, N$, as

$$q_m^j = D_m^{-1}(u_m^j), \tag{13}$$

where D_m^{-1} are inverse CDFs of D_m from Section 5.3.1. By construction, the correlation profile of annotation-degree vectors $\mathbf{q}_j$ is the same as of the ADD in the original topology, while the distributions of their components q_m^j are rescaled ADs.

Algorithm 1 lists the described low-level details of our multivariate rescaling, using the ADD as an example.

We conclude our discussion of rescaling with the following remark. Recall from the end of Section 4.2 that we have the following two types of multivariate statistics: the ADD and the JDDs. As illustrated in Figure 5, we rescale the ADD using all the three steps described in this section. For rescaling a JDD, it is not necessary to separately rescale its marginals, i.e., to use the first step of the described rescaling process, since the marginals of JDDs are distributions of scalar degrees that we automatically rescale during the ADD rescaling. To rescale a JDD, we execute only the second step of the described rescaling process to obtain the rescaled empirical JDD copula. We then use this copula to determine proper placement of edges in the final synthetic graph that we construct. In other words, the last, third step of our multivariate rescaling process applied to JDDs takes place during the graph construction phase, which we describe next.

Algorithm 1: Rescaling ADD

Input: Degree vectors $\mathbf{k}_i = (k_1^i, k_2^i, k_3^i)$, $i = 1 \dots n$, of the measured topology;
Input: Size N of the target synthetic topology.

```
// Step 1:  AD rescaling
```
forall $m = 1, 2, 3$ **do**
  Let k_m be the list of the m^{th} component values of vectors $\mathbf{k}_i$;
  Approximate distribution k_m by a smoothing spline S_m;
  Sample N numbers d_m^j, $j = 1 \dots N$, with probability distribution given by S_m;
  Let $D_m(d_m)$ be the CDF of d_m.
end

```
// Step 2:  copula rescaling
```
Re-sample N degree triplets $\mathbf{k}_j$ from the set of $\mathbf{k}_i$;
forall $m = 1, 2, 3$ **do**
  Let k_m be the list of the m^{th} component values of vectors $\mathbf{k}_j$;
  Sort list k_m in the non-degreasing order of values;
  forall $j = 1 \dots N$ **do**
    Let r_m^j be the position number of value k_m^j in the sorted list;
    $u_m^j = r_m^j/N$.
  end
end

```
// Step 3:  merge rescaled ADs and the ADD copula
```
forall $m = 1, 2, 3$ **do**
  forall $j = 1 \dots N$ **do**
    $q_m^j = D_m^{-1}(u_m^j)$.
  end
end

Output: Degree vectors $\mathbf{q}_j = (q_1^j, q_2^j, q_3^j)$, $j = 1 \dots N$, of the synthetic topology.

5.4 Construction

We describe the $1K$- and $2K$-annotated random graph constructors that are both generalizations of the well-known *configuration* or *pseudograph* approach in the terminology of [29]. The $1K$-constructor requires only the rescaled ADD, while the $2K$-constructor needs also the rescaled JDD copulas.

5.4.1 Constructing $1K$-annotated random graphs

Using the rescaled degree vectors $\mathbf{q}_j$, $j = 1 \dots N$, we construct $1K$-annotated random graphs using the following algorithm:

1. for each vector $\mathbf{q}_j = (q_1^j, q_2^j, q_3^j)$, prepare a node with q_1^j customer stubs, q_2^j provider stubs, and q_3^j peer stubs;
2. randomly select pairs of either customer-and-provider or peer-and-peer stubs, and connect (match) them together to form c2p or p2p links;
3. remove unmatched stubs, multiple edges between the same pair of nodes (loops), links with both ends connected to the same node (self-loops), and extract the largest connected component.

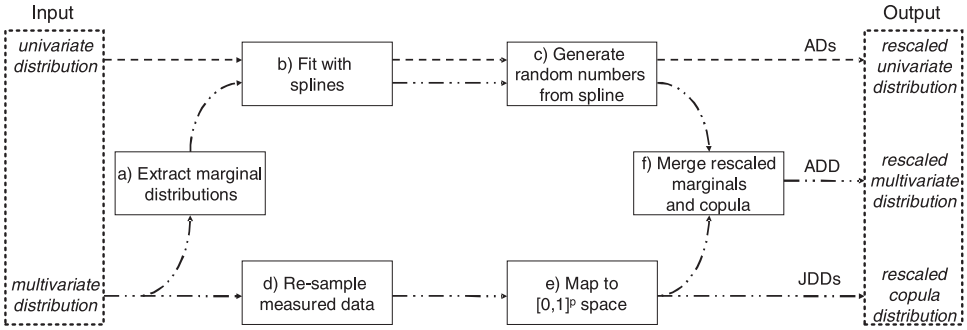

Figure 5: Overview of rescaling univariate and multivariate distributions.

The last step deals with the known problem of the pseudograph approach. As its name suggests, it does not necessarily produce simple connected graphs. In general, it generates pseudographs, i.e., graphs with (self-)loops, consisting of several connected components. The size of the largest connected component is usually comparable with the total pseudograph size, while all others are small. Extraction of this largest connected component and removal of all (self-)loops[6] alters the target degree distributions. Therefore, the resulting simple connected graph has a slightly different ADD than the one on the algorithm input.

Annotations alleviate this problem since they introduce a series of additional constraints. For example, in the non-annotated case, loops tend to form between high-degree ASs, simply because these ASs have a lot of stubs attached to them after step 1 of the algorithm. In the annotated case, the number of such loops is smaller because most stubs attached to high-degree ASs are annotated as provider stubs that can be matched only with customer stubs attached mostly to low-degree ASs.

Still, the $1K$-annotated random graphs are not perfect as, for example, p2p links might end up connecting nodes with drastically dissimilar degree, cf. the JDD discussion in Section 4.2. The $2K$-annotated random graphs do not have this problem.

5.4.2 Constructing $2K$-annotated random graphs

Earlier work [29] extends the pseudograph approach to non-annotated $2K$-distributions. We extend it even further for the $2K$-annotated case in the following algorithm:

1. for each vector $\mathbf{q}_j = (q_1^j, q_2^j, q_3^j)$, prepare a node with q_1^j customer stubs, q_2^j provider stubs, q_3^j peer stubs, and total degree $q^j = |\mathbf{q}_j|_1$;
2. determine the total numbers n_{c2p} and n_{p2p} of c2p and p2p edges in the target graph as the maximum possible number of customer-and-provider and peer-and-peer stubs that can be matched within the stub collection $\mathbf{q}_j$;
3. rescale the c2p and p2p JDD copulas[7] to target sizes of n_{c2p} and n_{p2p} degree pairs (q, q') corresponding to c2p and p2p edges between nodes of total degrees q and q' in the target graph;
4. for each c2p (or p2p) degree pair (q, q') select randomly a customer (or peer) stub attached to a node of degree q and a provider (or peer) stub attached to a node of degree q' and form a c2p (or p2p) edge;
5. use the procedure described below to rewire (self-)loops;
6. remove unmatched stubs, remaining (self-)loops, and extract the largest connected component.

The following rewiring procedure reduces the number of edges removed from the final graph. For each edge involved in a (self-)loop between nodes of degrees q_1 and q_2, we randomly select two non-adjacent nodes of degrees q_1 and q_2 and move the edge to these nodes. This procedure retains a large number of edges that would, otherwise, be removed from the graph. In theory, this procedure may skew the original $2K$-summary statistics. In practice, however, it alters these statistics negligibly.

The resulting graph has both the ADD and JDDs approximately the same as those obtained after rescaling. Minor discrepancies are due to the last step of the algorithm, but the number of (self-)loops and small connected components are even smaller than in the $1K$-annotated case. The reason for these improvements is yet additional structural constraints, compared with the $1K$-annotated case. For example, the JDD-induced constraints force the algorithm to create only one link between a pair of high-degree nodes, or no links between a pair of nodes of degree 1, thus avoiding creation of many connected components composed of such node pairs. The original graph does not have such links, and the rescaled JDDs preserve these structural properties, thus improving the resulting graph quality.

6. EVALUATION

In this section, we present results of evaluation of our $2K$-annotated graph generation method. We also evaluated the $1K$-annotated generator and found that, as expected, it produced less accurate graphs with defects such as those mentioned in Section 4.2, e.g., with p2p links connecting ASs of dissimilar degrees, etc.

Experiments. To evaluate the accuracy of our $2K$-annotated generator, we want to compare graphs it produces with the measured annotated Internet AS graph from Section 5.2. To simplify comparisons, we select one, most representative graph from a set of 50 random synthetic graphs. We select this most representative graph as follows. We first look for a simple graph metric that exhibits high variability

[6]Self-loops are removed, while multiple edges between the same pair of nodes are mapped to a single edge between the two nodes.

[7]See the remark at the end of Section 5.3.2.

across the generated graphs. One such metric is the maximum degree. The expected maximum degree in an n-node graph with a power-law degree distribution $P(k) \sim k^{-\gamma}$ is $k_{max} \approx n^{1/(\gamma-1)}$ [4]. Exponent γ is approximately 2.1 for the Internet AS topology. This value of γ stays constant as the Internet grows, and it implies almost linear scaling of the maximum degree since $1/(\gamma-1) \approx 0.9$, which is consistent with scaling of maximum degree in historical Internet topologies [36]. For these reasons, our most representative graph is the one with its maximum degree closest to its expected value, across all the generated graphs.

In addition, we evaluate the variance of important graph metrics described below, across ensembles of random graphs that we generate. Studying the variance properties of a graph generation technique is essential for estimating structural differences between equal-sized random graphs generated by the model, and for gaining insight on how such differences affect performance evaluation experiments. The variance properties of a graph generation technique is associated with the following tradeoff. On the one hand, variance should be small so that generated graphs closely match the observed topology. On the other hand, though, random graphs should not all be identical or almost identical, because if they do not exhibit sufficient structural diversity, then they have little value for performance evaluation studies. In our experiments, we compute and report the variance of important graph metrics in sets of 50 equal-sized random graphs.

Metrics. Since it is practically impossible to compare graphs over every existing graph metric, we select a set of metrics that were found particularly important in the Internet topology literature. These metrics include the degree distributions that we deal with in previous sections, assortativity coefficient, distance distribution, and spectrum. The *assortativity coefficient* is essentially the Pearson correlation coefficient of the joint degree distribution (JDD). Its positive (negative) values indicate that degrees of connected nodes are positively (negatively) correlated, meaning that nodes with similar (dissimilar) degrees interconnect with higher probabilities. The *distance distribution* is the distribution of lengths of the shortest paths in a graph, which we compute both with and without constraints imposed by annotations (routing policies). The *spectrum* of a graph is the set of the eigenvalues of its Laplacian L. The Laplacian's matrix elements L_{ij} are $-1/(k_i k_j)^{1/2}$ if there is an edge between node i of degree k_i and node j of degree k_j; 1 if $i = j$; and 0 otherwise. Among the n eigenvalues of L, the smallest non-zero and largest eigenvalues are most interesting, since they provide tight bounds to a number of important network properties. For more details on these and other metrics, and why they are important, see [30].

Results. In Figure 6 we plot the ADs of the measured AS topology and of the most representative synthetic graph of the equal size. We observe that the distributions of the customer, provider, and peer degrees in the synthetic graph are very close to the corresponding distributions in the measured topology. The close match demonstrates that: 1) spline-smoothing accurately models complex ADs of real Internet topologies, 2) random number generation yields empirical distributions that follow the modeled distributions, and 3) rewiring and removal of (self-)loops do not introduce any significant artifacts. It is, of course, expected that our generator accurately reproduces ADs, as they are part of the

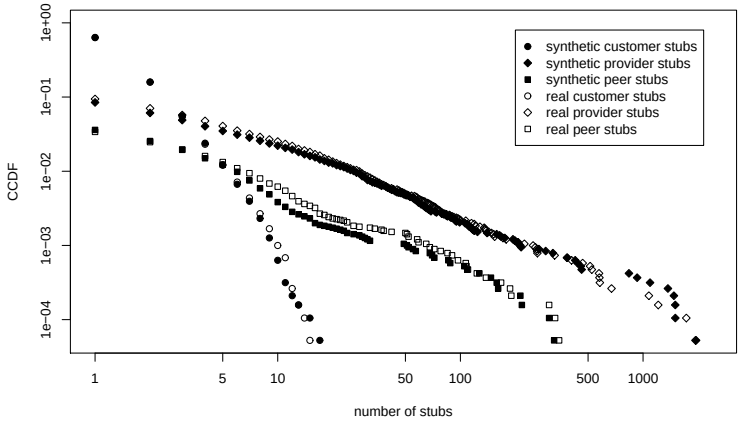

Figure 6: CCDFs of the number of customer, provider, and peer stubs in the synthetic versus measured AS topology.

$2K$-summary statistics we explicitly model. We also confirm that synthetic graphs, also as expected, closely reproduce all the other summary statistics that we explicitly model: the DD, ADD, and JDDs of the synthetic graph are very close to the originals. We do not show the corresponding plots for brevity.

In Figures 7(a) and 7(b) we compare the distance distributions of the measured and equal-sized synthetic topology ignoring and accounting for annotation-induced, i.e., routing policy, constraints. In the former case, we calculate lengths of the standard shortest paths between nodes in a graph as if the graph was non-annotated. In the latter case, we find lengths of shortest *valid*, i.e., valley-free, paths defined in Section 3. In both the non-annotated and annotated cases, we observe that the distance distribution in the synthetic graph closely matches the distance distribution in the measured topology, even though we have *not* explicitly modeled or tried to reproduce the distance distributions. We also observe that the distance distributions in the non-annotated and annotated cases are different, meaning that annotations in the synthetic graph properly filter realistic, policy-constrained paths from the set of all possible path in the non-annotated case.

In Table 3 we compare the measured topology with synthetic graphs of different sizes over a set of important scalar metrics, including those we do not explicitly model or try to reproduce, e.g., the eigenvalues of the Laplacian, etc. We compute these metrics for five synthetic graphs of sizes $5,000$, $10,000$, $30,000$, and $19,036$ nodes, the last size being equal to the size of the original topology. The first three metrics are the number of (c2p or p2p) edges in a graph. We observe that the number of such edges grows almost linearly with the number of nodes. This observation is consistent with that the average degree in historical Internet topologies stays almost constant [36]. The fourth metric is the maximum degree. As expected, the maximum degree grows with the size of the graph slightly slower than linearly. The next five metrics in the table describe properties that have stayed relatively constant in historical Internet topologies. These

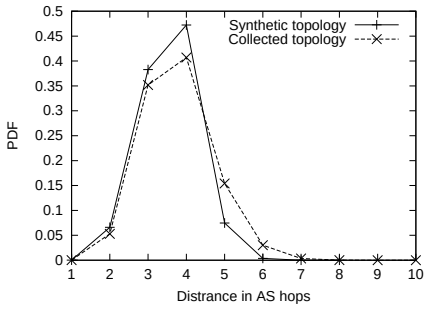

(a) Shortest paths.

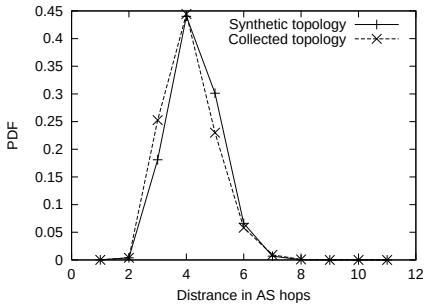

(b) Shortest *valid* paths.

Figure 7: Distance distributions in synthetic and measured AS topologies.

properties have small variations in the synthetic graphs as well.

Next we investigate the benefit of modeling the ADs and ADD in addition to the DD and JDDs. Previous work [29] shows that modeling DD and JDD is sufficient for capturing and reliably reproducing most important *non-annotated* graph metrics. The main value of modeling ADs and ADD is that our generated synthetic graphs are properly annotated. We saw in Section 3 that the Internet topology annotations are important. Here we provide another evidence that they are non-trivial. Specifically, in Figures 8(a), 8(b), and 8(c) we plot the total degrees of ASs in the measured AS topology versus their annotation degrees: the number of customers k_1, providers k_2, and peers k_3, respectively. We observe that a given total degree can correspond to a wide range of different values of k_1, k_2, and k_3. The JDD provides information only on total node degrees and on their correlations, whereas it is completely agnostic to annotation degrees. On the other hand, the ADs and ADD capture the distribution of annotation degrees and the correlations between annotation degrees, respectively. Therefore, the JDD alone is in principle incapable of capturing topology annotations, while the benefit of modeling ADs and ADD lies in reproducing realistic annotations in generated graphs.

To quantify the variance properties of randomly generated graphs, we compute the standard deviation of our metrics across sets of 50 random graphs. We construct 4 sets with topologies of 5,000, 10,000, 19,036, and 30,000 nodes, a total of 200 random graphs. Among our evaluation metrics, we do not compute the eigenvalues of the Laplacian and the assortativity coefficient, since they require prohibitively long computation times for 200 graphs. In Table 4, we show the standard deviation and mean value of the remaining metrics.

Table 4: Variance of graph metrics across sets of equal-sized random graphs.

graph metric	std. deviation / mean			
	5000 nodes	10000 nodes	19036 nodes	30000 nodes
c2p edges	399/17,905	267/36,876	349/71,055	410/112,549
p2p edges	100/1,238	203/2,980	396/6,412	541/12,863
max degree	387/1,618	417/2,090	471/2,335	376/2,599
av. degree	0.08/3.83	0.03/3.99	0.02/4.07	0.02/4.11
av. distance	0.13/3.16	0.09/3.40	0.10/3.61	0.06/3.77

The maximum degree exhibits the highest standard deviation (with respect to the mean) taking values between 376 and 471 for graphs of different size. The high variance of the maximum degree is expected, since the degree distribution of Internet topologies is highly skewed. On the other hand, the remaining metrics in Table 4 exhibit low variance. These metrics reflect aggregate graph properties and can be modeled as a sum of many i.i.d. random variables. Therefore, according to the central limit theorem, their distribution is approximately normal and their variance is consequently smaller than the variance of the maximum degree.

An important difference between the graph generation method described in this study and the graph generation methods described in our previous work [29] is that the former exhibits higher variance. The two methods are conceptually similar in generating synthetic graphs that reproduce the correlation profile of an observed topology—albeit [29] does not consider annotations. They differ in that our previous techniques directly use the degree distribution or correlations of an observed topology to generate new similar topologies. On the other hand, the present work first models the degree correlations of a topology and then uses random number generators to produce synthetic degree distributions fed into final graph constructors. In simpler words, our present technique induces more randomness by means of the synthetic generation of degree correlations based on the correlation profile extracted from the real topology. The two approaches are complementary and together provide a wider range of options for generating synthetic topologies with desired variance characteristics.

Overall, our evaluation results show that:

- $2K$-annotated random graphs generated with our approach faithfully reproduce a number of important properties of Internet topologies;
- rescaled graphs exhibit the expected behavior according to a number of definitive graph metrics, i.e., these metrics are either properly-rescaled or stay relatively stable as the size of synthetic graphs varies;
- the profile of correlations between annotation and total degrees is diverse; and
- random graphs generated with our method exhibit small variance, although higher than in our previous work [29].

7. CONCLUSIONS

In this work, we have focused on the problem of generating synthetic annotated graphs that model real complex networks. Our techniques are likely to have many applications not only in networking, but also in other disciplines

Table 3: Scalar metrics of synthetic and collected graphs. Note that smallest eigenvalues are positive, but some may round to zero.

Metric	Number of nodes				
	19036 (measured)	5000 (synthetic)	10000 (synthetic)	19036 (synthetic)	30000 (synthetic)
Number of edges	40115	10179	20730	39595	62853
Number of c2p edges	36188	9409	18917	36146	56870
Number of p2p edges	3927	770	1813	3448	5983
Maximum degree	2384	1014	1492	2385	3461
Average degree	4.21	4.07	4.15	4.16	4.19
Assortativity coefficient	-0.20	-0.30	-0.24	-0.25	-0.18
Largest eigenvalue of Laplacian	1.97	1.85	1.88	1.91	1.92
Smallest eigenvalue of Laplacian	0.03	0.00	0.12	0.09	0.00
Average distance	3.76	3.26	3.52	3.57	3.75

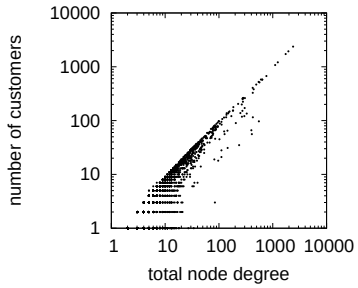

(a) Total degree vs. number of customers.

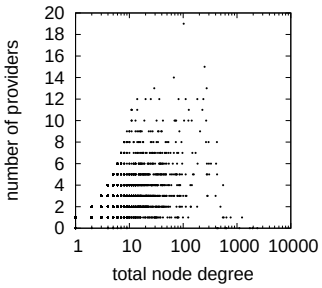

(b) Total degree vs. number of providers.

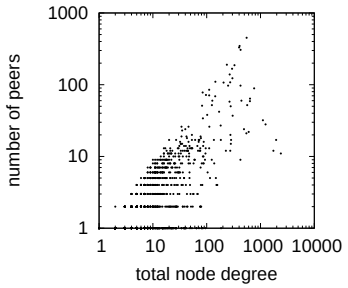

(c) Total degree vs. number of peers.

Figure 8: Scatterplots demonstrating the diversity of annotation degrees and that total node degrees are agnostic with respect to annotations.

where annotated graphs are used to abstract and represent network structure. For example, two groups have recently contacted us to discuss our techniques as they were searching for tools to generate synthetic, semantic-rich, i.e., annotated, networks for their simulation studies. The first group works on modeling the European powerline networks, while the second is in brain and neural network research. Other networks to which our techniques are immediately applicable include the router-level Internet, WWW, networks of critical resources dependencies, as well as many types of social and biological networks, such as regulatory pathways [35].

A number of open problems remain. In particular, our techniques construct synthetic versions of real topologies available from measurement projects. However, it is well-known that in many cases, the outcome of measurements does not accurately represent a real complete topology. In fact, there might exist inherent limitations in measuring certain network topologies with 100% accuracy. A venue for further research is the development of prediction techniques that extrapolate what we can presently measure in order to predict what we can not measure.

Another substantial problem is the difficulties in validating results of topology inference studies. For example, in the specific context of Internet topologies, validation is hard because of the unwillingness of service providers to release data on their infrastructure, network design, configuration, and performance. On the other hand, validation of any research result is a cornerstone to its reliability and utility. Therefore we believe it is imperative to focus on new validation techniques that would combine the limited ground truth data available today with convincing testbed or simulation experiments.

8. ACKNOWLEDGMENTS

This work was supported in part by NSF CNS-0434996 and CNS-0722070, by DHS N66001-08-C-2029, and by Cisco Systems.

9. REFERENCES

[1] W. Aiello, F. Chung, and L. Lu. A random graph model for massive graphs. In *STOC*, 2000.

[2] R. Albert and A.-L. Barabási. Topology of evolving networks: Local events and universality. *Phys Rev Lett*, 85(24):5234–5237, 2000.

[3] M. Boguñá and R. Pastor-Satorras. Class of correlated random networks with hidden variables. *Phys Rev E*, 68:036112, 2003.

[4] M. Boguñá, R. Pastor-Satorras, and A. Vespignani. Cut-offs and finite size effects in scale-free networks. *Eur Phys J B*, 38:205–209, 2004.

[5] M. Boguñá and M. A. Serrano. Generalized percolation in random directed networks. *Phys Rev E*, 72:016106, 2005.

[6] J. M. Carlson and J. Doyle. Highly optimized tolerance: A mechanism for power-laws in designed systems. *Phys Rev E*, 60:1412–1427, 1999.

[7] J. M. Chambers and T. J. Hastie. *Statistical Models in S*. Wadsworth and Brooks/Cole, Pacific Grove, California, 1992.

[8] H. Chang, S. Jamin, and W. Willinger. To peer or not to peer: Modeling the evolution of the Internet's AS-level topology. In *INFOCOM*, 2006.

[9] F. Chung and L. Lu. Connected components in random graphs with given degree sequences. *Ann Comb*, 6:125–145, 2002.

[10] A. Clauset and C. Moore. Accuracy and scaling phenomena in Internet mapping. *Phys Rev Lett*, 94:018701, 2005.

[11] L. Dall'Asta, I. Alvarez-Hamelin, A. Barrat, A. Vázquez, and A. Vespignani. Exploring networks with traceroute-like probes: Theory and simulations. *Theor Comput Sci, Complex Networks*, 355(1):6–24, 2006.

[12] C. de Launois. GHITLE: Generator of Hierarchical Internet Topologies using LEvels. `http://ghitle.info.ucl.ac.be/`.

[13] X. Dimitropoulos, D. Krioukov, M. Fomenkov, B. Huffaker, Y. Hyun, kc claffy, and G. Riley. AS relationships: Inference and validation. *Comput Commun Rev*, 37(1), 2007.

[14] X. Dimitropoulos, D. Krioukov, B. Huffaker, kc claffy, and G. Riley. Inferring AS relationships: Dead end or lively beginning? In *WEA*, 2005.

[15] X. Dimitropoulos, D. Krioukov, G. Riley, and kc claffy. Revealing the Autonomous System taxonomy: The machine learning approach. In *PAM*, 2006.

[16] X. Dimitropoulos and G. Riley. Creating realistic BGP models. In *MASCOTS*, 2003.

[17] M. Doar. A better model for generating test networks. In *GLOBECOM*, 1996.

[18] P. Erdős and A. Rényi. On random graphs. *Publ Math*, 6:290–297, 1959.

[19] M. Faloutsos, P. Faloutsos, and C. Faloutsos. On power-law relationships of the Internet topology. In *SIGCOMM*, 1999.

[20] O. Frank and D. Strauss. Markov graphs. *J Am Stat Assoc*, 81(395):832–842, 1986.

[21] L. Gao. On inferring Autonomous System relationships in the Internet. *IEEE ACM T Network*, 9(6), 2001.

[22] L. Gao and F. Wang. The extent of AS path inflation by routing policies. In *Global Internet*, 2002.

[23] C. Gkantsidis, M. Mihail, and E. Zegura. The Markov chain simulation method for generating connected power law random graphs. In *ALENEX*, 2003.

[24] E. Hewitt. *Real and Abstract Analysis: A Modern Treatment of the Theory of Functions of a Real Variable*. Springer Verlag, 1975.

[25] W. Hörmann, J. Leydold, and G. Derflinger. *Automatic Nonuniform Random Variate Generation*. Springer-Verlag, Berlin, 2004.

[26] D. Krioukov, kc claffy, K. Fall, and A. Brady. On compact routing for the Internet. *Comput Commun Rev*, 37(3):41–52, 2007.

[27] A. Lakhina, J. Byers, M. Crovella, and P. Xie. Sampling biases in IP topology measurements. In *INFOCOM*, 2003.

[28] L. Li, D. Alderson, W. Willinger, and J. Doyle. A first-principles approach to understanding the Internets router-level topology. In *SIGCOMM*, 2004.

[29] P. Mahadevan, D. Krioukov, K. Fall, and A. Vahdat. Systematic topology analysis and generation using degree correlations. In *SIGCOMM*, 2006.

[30] P. Mahadevan, D. Krioukov, M. Fomenkov, B. Huffaker, X. Dimitropoulos, kc claffy, and A. Vahdat. The Internet AS-level topology: Three data sources and one definitive metric. *Comput Commun Rev*, 36(1):17–26, 2006.

[31] S. Maslov, K. Sneppen, and A. Zaliznyak. Detection of topological patterns in complex networks: Correlation profile of the Internet. *Physica A*, 333:529–540, 2004.

[32] A. Medina, A. Lakhina, I. Matta, and J. Byers. BRITE: An approach to universal topology generation. In *MASCOTS*, 2001.

[33] R. B. Nelson. An introduction to copulas. *Springer-Verlag Lecture Notes in Statistics*, 139:216, 1999.

[34] C. Palmer and G. Steffan. Generating network topologies that obey power laws. In *GLOBECOM*, November 2000.

[35] J. Pandey, M. Koyuturk, Y. Kim, W. Szpankowski, S. Subramaniam, and A. Grama. Functional annotation of regulatory pathways. *Bioinformatics*, 23(13):i377–i386, 2007.

[36] R. Pastor-Satorras and A. Vespignani. *Evolution and Structure of the Internet: A Statistical Physics Approach*. Cambridge University Press, Cambridge, 2004.

[37] The R Project for Statistical Computing. `http://www.r-project.org/`.

[38] University of Oregon RouteViews Project. `http://www.routeviews.org/`.

[39] A. Sklar. Fonctions de répartition à n dimensions et leures marges. *Publications de l'Institut de Statistique de L'Université de Paris*, 8:229231, 1959.

[40] B. Söderberg. A general formalism for inhomogeneous random graphs. *Phys Rev E*, 66:066121, 2002.

[41] B. Söderberg. Properties of random graphs with hidden color. *Phys Rev E*, 68:026107, 2003.

[42] B. Söderberg. Random graphs with hidden color. *Phys Rev E*, 68:015102(R), 2003.

[43] B. Söderberg. Random Feynman graphs. In *AIP Conf Procs*, volume 776, pages 118–132, 2005.

[44] B. M. Waxman. Routing of multipoint connections. *JSAC*, 1988.

[45] J. Winick and S. Jamin. Inet-3.0: Internet topology generator. Technical Report UM-CSE-TR-456-02, University of Michigan, 2002.

[46] E. W. Zegura, K. Calvert, and S. Bhattacharjee. How to model an internetwork. In *INFOCOM*, 1996.